Supporting information

Surface Group-Governed Charge Storage in Carbon Dots for a Visual Memristor

Dongren Zheng,[a] Tianyang Zhang,[a] Haizhou Yu,[a] Xiangyong Meng,[a] Zhongshan Yang,[b] Hui Huang,[a] Yang Liu*[a] and Zhenhui Kang *[a,b]

[a]State Key Laboratory of Bioinspired Interfacial Materials Science, Institute of Functional Nano & Soft Materials (FUNSOM), Soochow University, Suzhou, 215123, Jiangsu, China.

E-mails: yangl@suda.edu.cn; zhkang@suda.edu.cn

[b]Macao Institute of Materials Science and Engineering (MIMSE), MUST−SUDA Joint Research Center for Advanced Functional Materials, Macau University of Science and Technology, Taipa 999078, Macao, China.

Email: zhkang@suda.edu.cn

Supplementary Information

1. **Supplementary Text**

2. **Supplementary Figures 1 to 14**

3. **Supplementary Table 1 to 2**

Supplementary Text

1. Materials

Citric acid and cysteamine were purchased from Sinopharm. Poly(9-vinylcarbazole) (PVK) was purchased from Xi'an Polymer Light Technology company. Ethanol was purchased from Sinopharm. All chemicals were used as received without further purification unless otherwise specified.

2. Synthesis of carbon dots

Carbon dots (CDs) were synthesized via a one-step hydrothermal method. Specifically, 200 mg citric acid and 16 mg cysteamine were dispersed in 15 mL ethanol. The mixture was then transferred into 20 mL hydrothermal autoclave and heated at 200 °C for 3 h to obtain CDs.

3. Device fabrication

Briefly, indium tin oxide (ITO)-coated glass substrates were sequentially ultraso nically cleaned in acetone, a commercial ITO glass cleaning solution, and etha nol for 30 min each. After drying, the substrates were treated by ozone clea ning to remove residual organic contaminants and to increase the work functi on of ITO, thereby reducing the hole-injection barrier in the optoelectronic de vices.

A PEDOT:PSS layer was then spin-coated onto the cleaned ITO substrates at 4000 rpm for 40 s, followed by thermal annealing at 130 °C for 10 min. Sub sequently, a mixed solution of poly(9-vinylcarbazole) (PVK) and carbon dots (C Ds) with a mass ratio of 4:1 was spin-coated onto the PEDOT:PSS layer at 1

500 rpm for 40 s, and the resulting film was annealed at 100 °C for 100 min to ensure sufficient solvent evaporation and film uniformity.

The top electrodes were deposited using a thermal evaporation system under high vacuum. Specifically, TPBi (20 nm) was first deposited at a rate of 0.5 Å s^{-1} under a current of 33 A, followed by deposition of Liq (2 nm) at 0.1 Å s^{-1}, and finally Al (100 nm) at a rate of 2 Å s^{-1}. The multilayer deposition was carried out sequentially without breaking vacuum to ensure clean interfaces and good device reproducibility.

Electrical Measurements: At room temperature and in the atmosphere, the direct current (DC) and pulse characteristics of the device were measured using a Keithley SCS4200 semiconductor parameter analyzer. For pulse measurements, the list mode of the SMU module was employed, as the system is not equipped with a PMU module.

Materials characterizations: The morphology of CDs, including TEM and HRTEM images, was observed by TEM (FEI TF20) with the acceleration voltage of 200 kV. The XRD patterns were obtained by an X-ray powder diffractometer (Empyrean, Holland Panalytical) with Cu Kα radiation (λ = 0.15406 nm). The XPS data were measured by X-ray photoelectron spectroscopy (Thermo Kalpha) with Al Kα radiation of 1486 eV and all the XPS data were checked according to the C 1s binding energy of 284.6 eV. The FTIR spectra were acquired by Fourier transform micro infrared spectrometer (VERTEX 70). The Raman spectra

were measured through laser confocal micro-Raman spectrometer (LabRam HR Evolution). The UV-vis absorption spectra were obtained by UV/vis/NIR spectroph otometer (Lambda750, PerkinElmer). The PL spectra were measured by Hitachi F-4600 fluorescence spectrophotometer and TRPL spectra were obtained throu gh the same device applied a 370 nm pulsed laser working as the exciting li ght source. The PLQY was measured by the C9920-02G (HAMAMATSU) with a n integrating sphere. The UPS data are acquired by ultraviolet photoelectron spectrometer with an unfiltered He I (21.22 eV) gas discharge lamp and a to tal instrumental energy resolution of 100 MeV. The CV curves were measured by CHI 760D electrochemical workstation with a standard three-electrode syst em. The EL spectra, curves of the voltage versus current density and the lum inance were all measured by a photometer (Photo Research PR 655 spectrop hotometer) which was adhered to the constant current source (Keithley 2400s Source Meter).

4. Bandgap calculation

Plot with *hv* as X and dln(α*hv*)/dln(*hv*) as Y. The X corresponding the maximum value of Y is E_g. The derivation process is shown as follows:

$$\alpha hv = \mathrm{A}\left(hv - E_g\right)^n$$

$$\text{let} \quad y = \alpha hv,\ x = hv; \quad y = \mathrm{A}\left(x - E_g\right)^n$$

$$\ln y = \ln A - n\ln\left(x - E_g\right)$$

$$X = E_g \quad ; \quad \frac{d\ln y}{\ln x} \to \infty$$

Supplementary Figures

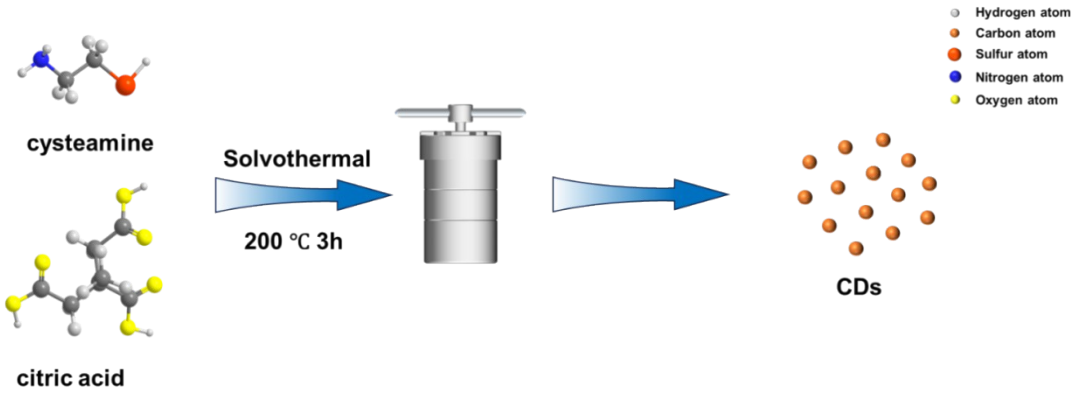

Figure S1. Schematic diagram of CDs synthesis process.

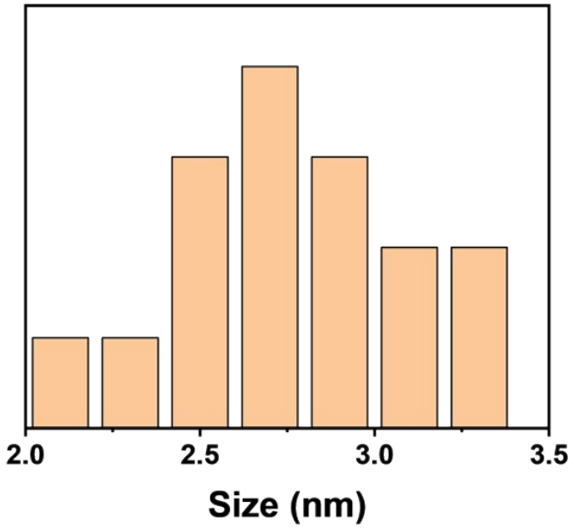

Figure S2. The size distributions of CDs.

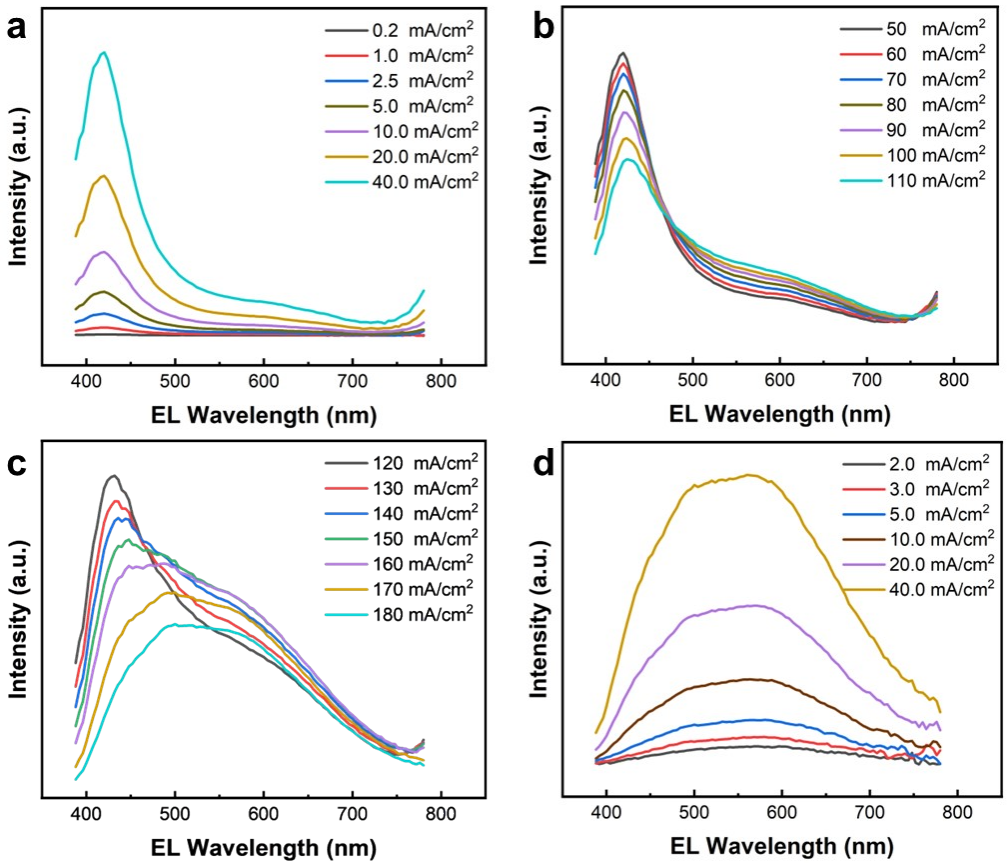

Figure S3. Electroluminescence spectra of CDs-based device. (a) Current density ranging from 0.2-40 mA/cm^2. (b) Current density ranging from 50-110 mA/cm^2. (c) Current density ranging from 120-180 mA/cm^2. (d) Re-illuminated EL spectr ranging from 50-110 mA/cm^2.

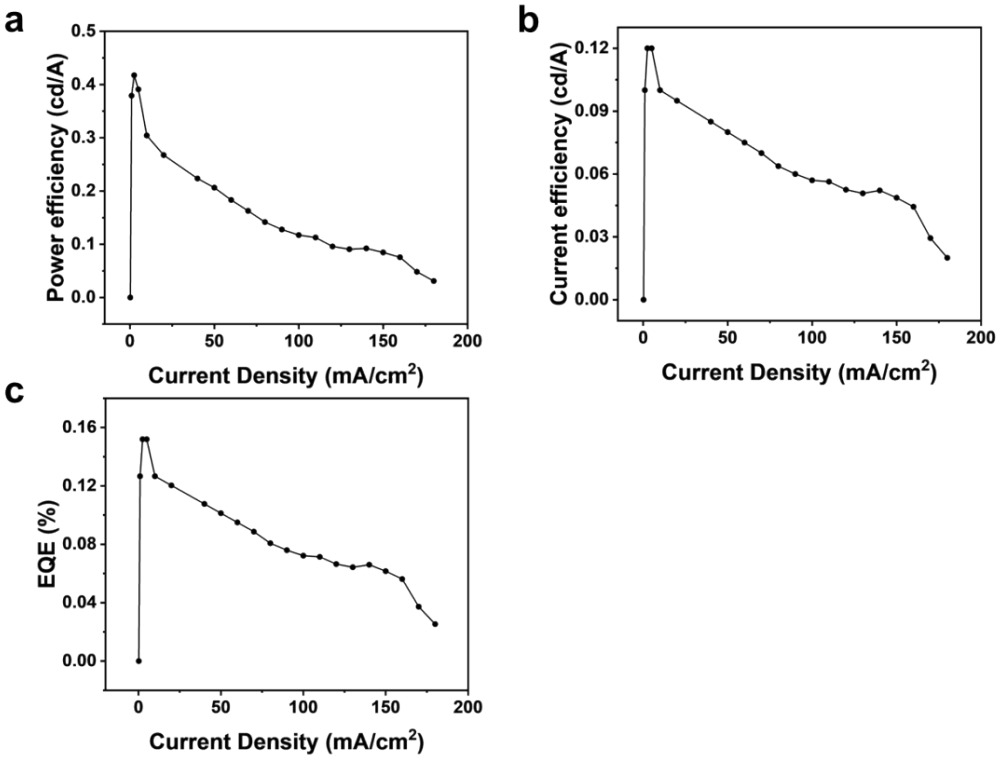

Figure S4. (a) The relationship between power efficiency and current density of devices. (b) The relationship between current efficiency and voltage of devices. (c) The relationship between external quantum efficiency and voltage.

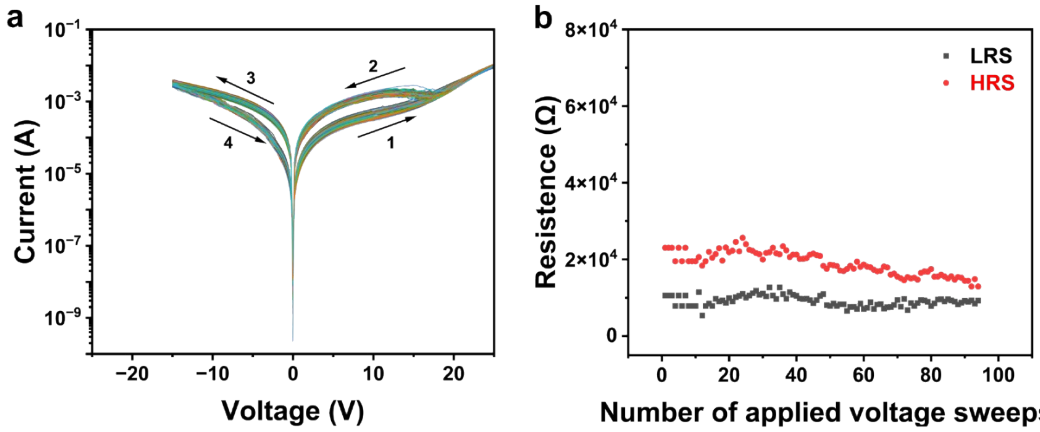

Figure S5. (a) I–V curves of the device over 94 consecutive cycles. (b) Distribution of high and low resistance states under 94 cycles.

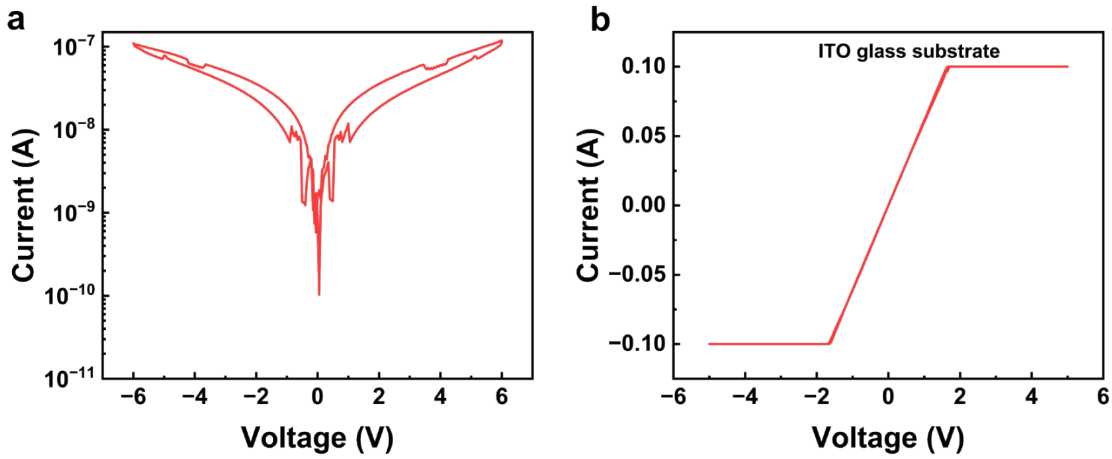

Figure S6. (a) Cyclic I–V curves of the device (-6 V-6 V). (b) Current-Voltage (I-V) Curves of ITO Glass Substrate with an Instrument Current Limit of 0.1 A.

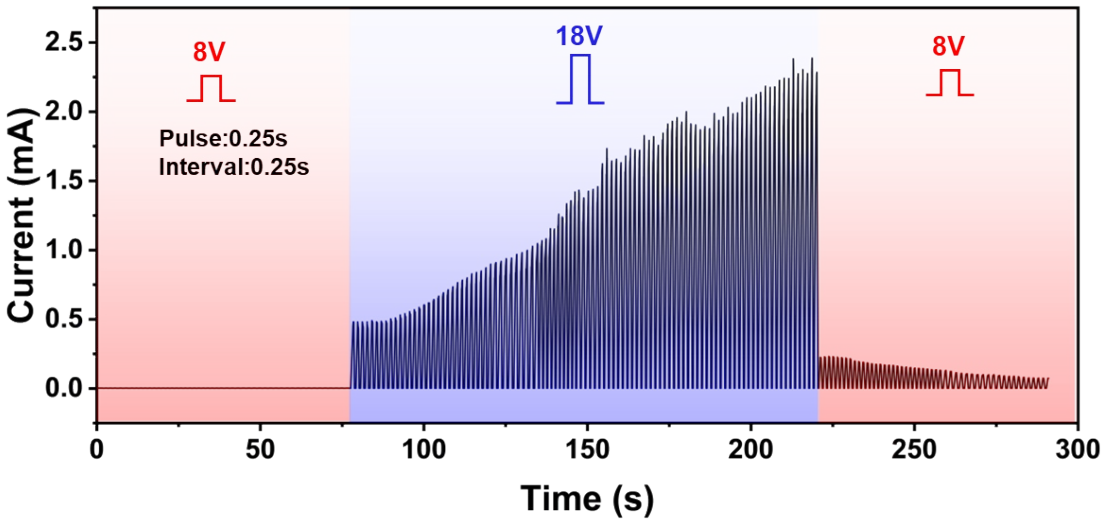

Figure S7. Long-term synaptic potentiation of the device under 130 pulsed voltage stimulation, a pulse group comprises a potentiation pulse train (8 V, red area) and a retention pulse train (18 V, blue area), Both pulse width and pulse interval are 0.25 s.

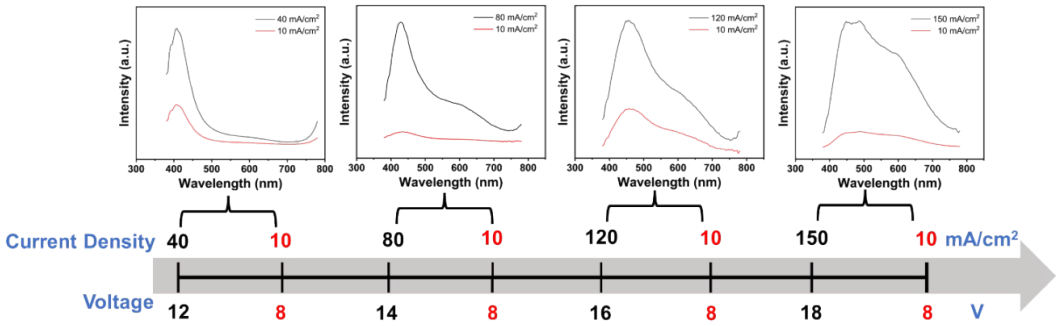

Figure S8. EL spectra of devices at different current densities and corresponding voltages.

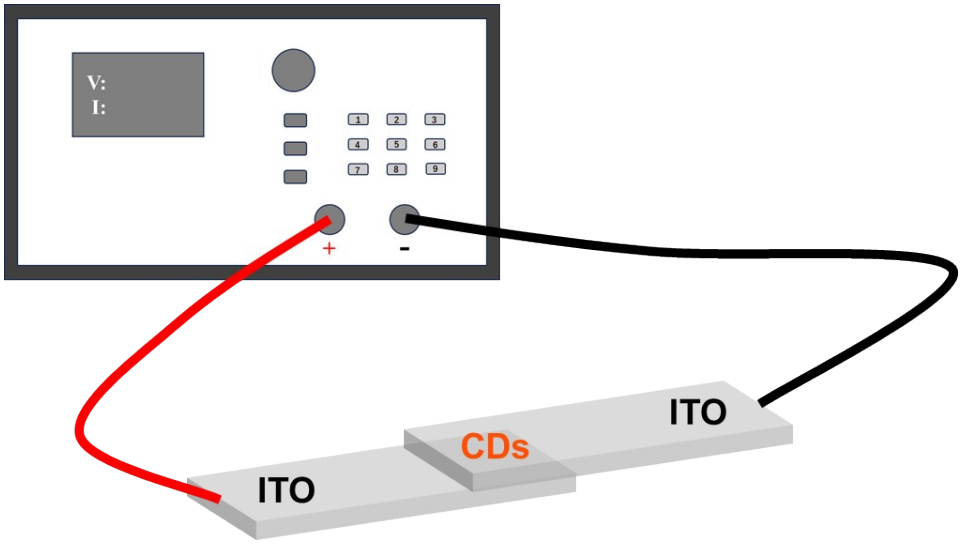

Figure S9. The diagrammatic sketches for electrical treatment.

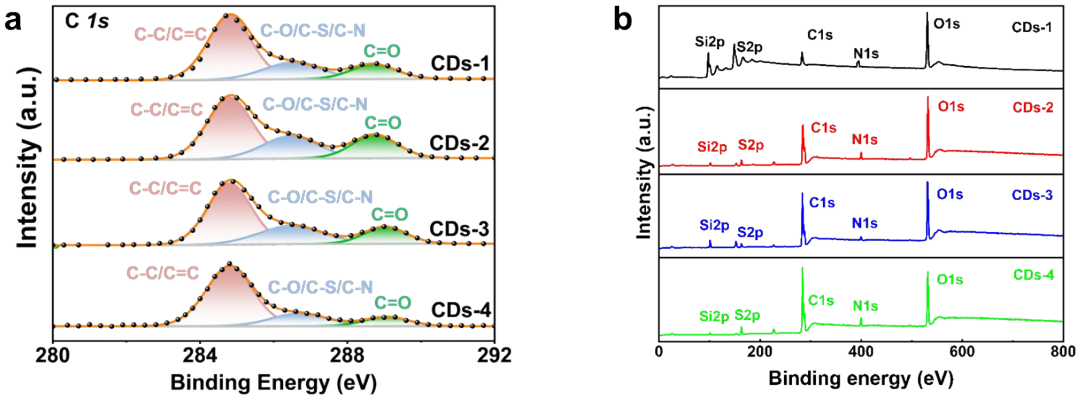

Figure S10. (a) High-resolution XPS spectra of C 1s for CDs 1-4. (b) The full XPS survey spectra of CDs subjected to four different electrical treatments

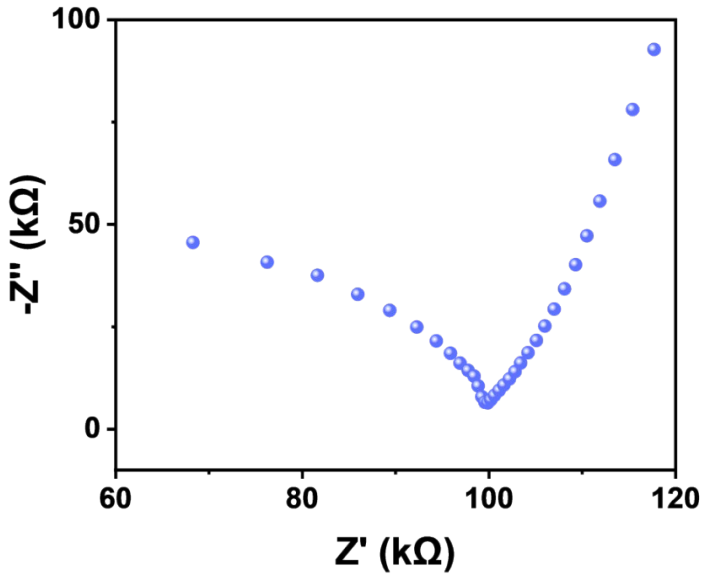

Figure S11. EIS spectrum of the original CDs.

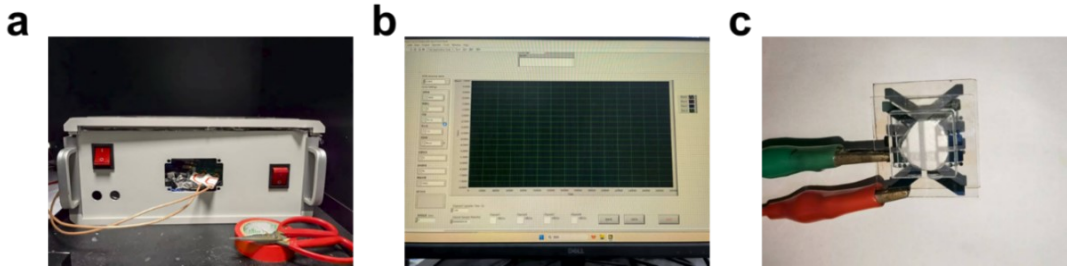

Figure S12. (a) Photograph of the TPS device. (b) Software interface for testing. (c) Photograph of the device testing setup and the clamping position of the test fixture.

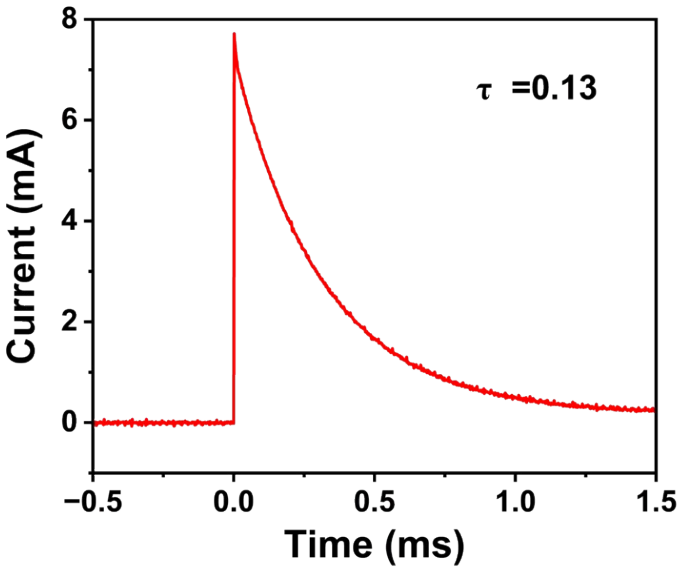

Figure S13. Current decay curve of the device after the application of reset voltage.

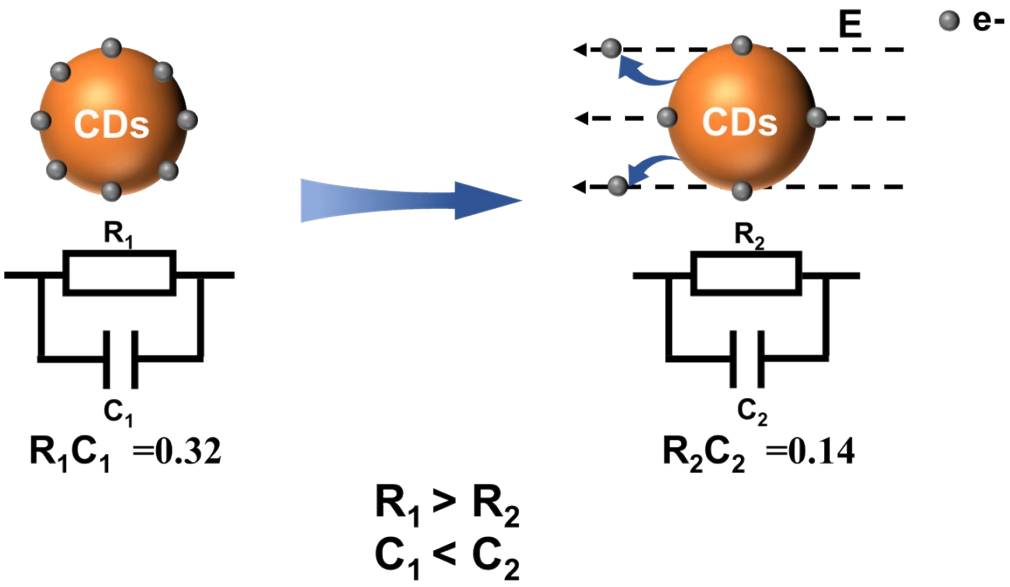

Figure S14. Schematic diagram of *in-situ* release of electrons by the device before and after reverse voltage application.

Supplementary Table

Table S1. Summary of the key parameters of some representative memristors reported in recent literatures.

Device	Visual output	Optical–electrical coupling	Operating voltage	Reference
Ag/AgInSbTe/a-Si/Pt	No	none	low	2021[1]
Cu/NbSe2/Au	No	none	low	2024[2]
Cu/a-Nb2O5/Au	No	none	low	2023[3]
Au/a-ZATO/Au	No	none	low	2023[4]
Al/LIQ/TPBI/CDs/PVK/PEDOT:PSS/ITO	Yes	Strongly coupled	high	This work

Table S2. The sample handling for mechanism exploration.

Serial Number	Handling Method	Time
CDs-1	Electrifying 0.5 V	1 min
CDs-2	Electrifying 10 V	1 min
CDs-3	Electrifying 15 V	1 min
CDs-4	Electrifying 20 V	1 min

References

1. Y. Ren, X. Fu, Z. Yang, R. Sun, Y. Lin, X. Zhao, Z. Wang, H. Xu and Y. Liu, *Applied Physics Letters*, 2021, **118**.
2. B. Lu, D. Hu, R. Yang, J. Du, L. Hu, S. Li, F. Wang, J. Huang, P. Liu, F. Zhuge, Y.-J. Zeng, Z. Ye and J. Lu, *SmartMat*, 2024, **5**, e1240.
3. S. Li, J. Du, B. Lu, R. Yang, D. Hu, P. Liu, H. Li, J. Bai, Z. Ye and J. Lu, *Materials Horizons*, 2023, **10**, 5643-5655.
4. B. Lu, J. Du, J. Lu, S. Li, R. Yang, P. Liu, J. Huang, L. Chen, F. Zhuge and Z. Ye, *ACS Materials Letters*, 2023, **5**, 1350-1358.